

Synthesis and Study of Structural, Optical Properties of $\text{Co}_x\text{Zn}_{1-x}\text{S}$ Semiconductor Compounds.

V. Laxmi Narasimha Rao¹, T. Shekharam, K. Hadasa, G. Yellaiah and
M. Nagabhushanam².

Department of Physics, University College of Science, Osmania University, Hyderabad-500 007, India

Abstract: $\text{Co}_x\text{Zn}_{1-x}\text{S}$ ($x=0-0.1$) polycrystalline semiconductor compounds were synthesised by co-precipitation method and were characterised by X-ray diffraction (XRD), UV-absorption, EDAX, SEM and Fourier Transform Infrared (FTIR) studies. XRD studies have shown that these powders have polycrystalline nature with a gradual variation from hexagonal to cubic structure while x changing from 0 to 0.1. UV-absorption studies revealed that the band gap of $\text{Co}_x\text{Zn}_{1-x}\text{S}$ ($x=0-0.1$) samples decreased with increase in cobalt concentration, owing to the enhancement of $sp-d$ exchange interactions and typical $d-d$ transitions. Chemical homogeneity and surface morphology studies were carried out by using EDAX and SEM. Fourier Transform Infrared (FTIR) spectroscopy also revealed that cobalt is induced into the lattice replacing Zinc.

Keywords: Polycrystalline Semiconductor $\text{Co}_x\text{Zn}_{1-x}\text{S}$, X-ray Diffraction, EDAX, SEM, Optical Properties.

I. Introduction

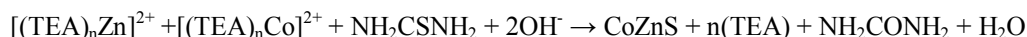
Semiconductor compounds prepared in the nano form have attracted considerable attention over the past decade because of their novel electric and optical properties [1] originating from quantum confinement effects. These quantum confinement effects make these materials behave remarkably different and they are observed in materials prepared by employing special conditions and this has stimulated much research interest. The existing semiconductor devices utilise the charge of an electron, the spin remaining unexploited. Diluted Magnetic Semiconductors (DMS) provide an opportunity to control both charge and spin of an electron and pave way for 'Spintronic Devices' [2], which promises to higher speeds, lower power consumption and higher integration devices [3,4]. DMS are semiconducting compounds in which a fraction of nonmagnetic cations are substituted by magnetic transitional metal or rare earth metal ions such as Mn, Fe, Co, Cr, Ni, Sm, Er, Gd etc., [5-7]. The development of magnetic semiconductors with practical ordering temperatures could lead to a new class of devices and circuits, including spin transistors and ultradense nonvolatile semiconductor memory [8].

As a wide-gap II-IV compound semiconductor, ZnS has been extensively studied due to its wide applications as phosphors [9], optical sensors and photocatalysts in environmental protection [10-12]. Sphalerite, the cubic (zincblende) structure of ZnS is stable at room temperature, while wurtzite, the dense hexagonal structure, is stable above 1020°C at atmospheric pressure and metastable as a microscopic phase under ambient conditions [13]. Doped ZnS nanocrystals have potential to form a new class of luminescent materials, high active photocatalysts [14] and diluted magnetic semiconductors (DMS) [15-17]. Sphalerite ZnS doped with Mn, Cu, Ag, Ni and Co have been synthesized [18-20] and their physical properties have been studied extensively. However, there are few reports regarding to the preparation and characterisation of wurtzite ZnS doped with transition metal ions, which are very difficult to be synthesized in solution at about room temperature [21, 22]. Recently, synthesis of pure wurtzite ZnS nanostructures by solvothermal reaction have been reported [22]. However, the literature survey reveals, that there is no work on the preparation and characterisation of bulk $\text{Co}_x\text{Zn}_{1-x}\text{S}$ semiconductor compound. In view of this the present study on $\text{Co}_x\text{Zn}_{1-x}\text{S}$ polycrystalline bulk semiconductor material prepared by chemical co-precipitation method. The advantage of this method is simple and low-cost. In this paper we report cobalt doped wurtzite ZnS semiconductor, as an important member in the family of ZnS based DMSs, and its structural and optical studies.

II. Experimental

Mixed $\text{Co}_x\text{Zn}_{1-x}\text{S}$ ($x=0, 0.02, 0.04, 0.06, 0.08, 0.1$) semiconductor powders were prepared by controlled co-precipitation method. In this method equimolar (1 mole) solution of high pure (AR grade) Cobalt Acetate, Zinc Acetate, Thiourea and Triethanolamine (TEA), were prepared using double distilled water and were mixed proportionately. The preparation process is based on the slow release of Co^{2+} , Zn^{2+} and S^{2-} ions in the solution. The ions condense on an ion-ion basis in the solution. The slow release of $\text{Co}^{2+}/\text{Zn}^{2+}$ ion is achieved by the dissociation of a complex species of Co/Zn such as the tetramine Co-II $[\text{Co}(\text{NH}_3)]^{2+}_4$ or tetramine Zinc-II $[\text{Zn}(\text{NH}_3)]^{2+}_4$ complex. The S^{2-} ions are supplied by the decomposition of an organic sulfur compound such as thiourea.

During this process, the chemistry involved for the formation of CoZnS from the reagents used can be written as [23],



The chemical reaction to form the specific composition $\text{Co}_x\text{Zn}_{1-x}\text{S}$ can be written as,



After the completion of the reaction the compound appears in the form of precipitate. The dried precipitate was treated and transformed into pellets of 1.5 cm diameter and 1.5 mm thickness under pressure. The details of the pre treatment are explained in our paper [24]. The pellets were annealed at 800 °C for 2 hours under the Nitrogen atmosphere. The pressure of the flowing gas was maintained uniform throughout the heating process and the furnace was cooled very slowly (1 °C/ minute) to room temperature.

The X-ray diffractograms of all the samples were obtained with BRUKER AXS D8 X-ray diffractometer with Cu- α radiation of wavelength 1.5406 Å, the optical absorption was recorded using SHIMADZU, UV-3100. SEM and Elemental analysis was carried out by using ZEISS EVO-18.

III. Results and Discussion

3.1 Structural Analysis

The structural analysis of $\text{Co}_x\text{Zn}_{1-x}\text{S}$ ($x=0-0.1$) compound was carried out by using X-ray diffractometer in the angular range from 20° to 80°. Fig. 1 shows the XRD patterns of $\text{Co}_x\text{Zn}_{1-x}\text{S}$ compound as a function of Cobalt concentration (x). The prominent diffraction peak is originated at $2\theta=28.537^\circ$ ($d=0.31508$ nm). Further, the XRD results show that all the compounds with $x=0-0.1$ have polycrystalline nature. The results of all the compounds are compared with the JCPDS data and found that, they match with the hexagonally structured ZnS (Card No.892347). And also it is found that the prominent peaks of hexagonal structure match with the main peak of cubic ZnS structure (Card No. 651691). Therefore, it is understood that the $\text{Co}_x\text{Zn}_{1-x}\text{S}$ compounds with $x=0-0.08$ have both cubic and hexagonal phases. But the compound with $x=0.1$ is found to have prominent peaks corresponded with cubic phase and remaining peaks present in the compound were almost having very less intensity. Hence, it is understood that the hexagonal phase is getting suppressed as cobalt concentration (x) in $\text{Co}_x\text{Zn}_{1-x}\text{S}$ reaches 0.1. It is also observed from the diffractograms that, the intensities of the prominent peaks ($d=3.150$, 1.911 and 1.634Å) remained almost the same, whereas the intensities of other peaks gradually decreased with the increase in the concentration of cobalt ($x=0-0.1$). The observed peaks are assigned miller indices as per the JCPDS data and the lattice parameters are calculated (Table 1).

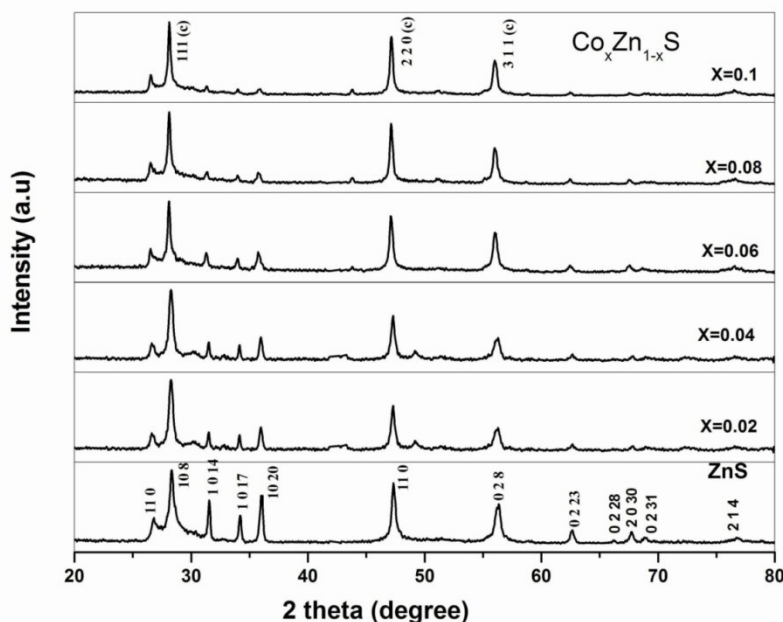


Fig 1. XRD diffractograms of $\text{Co}_x\text{Zn}_{1-x}\text{S}$ ($x=0-0.1$) compound.

TABLE 1. The d values, (hkl) miller indices of $\text{Co}_x\text{Zn}_{1-x}\text{S}$ (x=0-0.1) compound.

d values of ZnS Hexagonal structure JCPDS Card No.892347		Observed d values of $\text{Co}_x\text{Zn}_{1-x}\text{S}$ (x=0-0.08)	d values of ZnS Cubic structure JCPDS Card No.651691		Observed d values of $\text{Co}_x\text{Zn}_{1-x}\text{S}$ (x=0.1)
(h,k,l) values	d (Å)	d (Å)	(h,k,l) values	d (Å)	d (Å)
(1 0 0)	3.31	3.328
(1 0 8)	3.124	3.151	(1 1 1)	3.123	3.121
(1 0 14)	2.816	2.835	(2 0 0)	2.705	...
(1 0 17)	2.647	2.622
(1 0 20)	2.481	2.479
(1 1 0)	1.911	1.911	(2 2 0)	1.913	1.911
(0 2 8)	1.631	1.634	(3 1 1)	1.631	1.632
(0 2 23)	1.476	1.474	(2 2 2)	1.561	...
(0 2 28)	1.408	1.403
(2 0 30)	1.38	1.381
(0 2 31)	1.366	1.362	(4 0 0)	1.352	...
(2 1 4)	1.242	1.239	(3 3 1)	1.241	...

The lattice parameters *a* and *c* of the unit cell for the hexagonal and *a* for the cubic structures were calculated according to the relations [25].

$$\frac{1}{d^2_{hkl}} = \frac{4}{3} \left(\frac{h^2+hk+k^2}{a^2} \right) + \frac{l^2}{c^2} \quad (\text{for hexagonal}) \quad (7)$$

$$\frac{1}{d^2_{hkl}} = \left(\frac{h^2+k^2+l^2}{a^2} \right) \quad (\text{for cubic}) \quad (8)$$

The structural parameters such as grain size (D), dislocation density (δ), and micro strain (ϵ) for all the compositions are evaluated from XRD patterns using the following expressions. The average grain size was calculated from XRD patterns using Debye Scherrer's formula [26].

$$D = \frac{0.94\lambda}{\beta \cos\theta} \quad (9)$$

Where λ is the X-ray wavelength, θ is the diffraction angle and β is FWHM of the peak. The dislocation density (δ) was calculated by the formula [26].

$$\delta = \frac{1}{D^2} \quad (10)$$

The strain values were calculated from the following relation [27].

$$\epsilon = \frac{\beta \cos\theta}{4} \quad (11)$$

The calculated values of grain size (D), dislocation density (δ) and strain (ϵ) are presented in Table 2. As can be seen from Table 2, the grain size increase, whereas the dislocation density and strain decrease with the increase in cobalt concentration(x). These changes may be attributed to the improvement in the crystallinity of the compound [26]. It may be noted that the variation of D, δ and ϵ with cobalt concentration is non-linear and is shown in Fig. 2(a,b,c).

TABLE 2. The lattice parameters “*a*” nm, “*c*” nm values, average grain size (D), dislocation density (δ), FWHM (β), and micro strain (ϵ) for all the compositions of $\text{Co}_x\text{Zn}_{1-x}\text{S}$ (x=0-0.1) compound.

$\text{Co}_x\text{Zn}_{1-x}\text{S}$	<i>a</i> (nm)	<i>c</i> (nm)	FWHM(β)	(D) nm	(δ) $\times 10^{-3}$ (nm ⁻²)	(ϵ) $\times 10^{-2}$ (line ⁻² m ⁻⁴)
ZnS	0.3820	7.542	0.411	30.59	1.07	9.93
$\text{Co}_{0.02}\text{Zn}_{0.98}\text{S}$	0.3824	7.488	0.315	31.09	1.03	7.81
$\text{Co}_{0.04}\text{Zn}_{0.96}\text{S}$	0.3822	7.538	0.288	34.86	0.83	7.43
$\text{Co}_{0.06}\text{Zn}_{0.94}\text{S}$	0.3821	7.523	0.276	38.90	0.67	6.76
$\text{Co}_{0.08}\text{Zn}_{0.92}\text{S}$	0.3824	7.531	0.245	39.23	0.62	5.91
$\text{Co}_{0.1}\text{Zn}_{0.9}\text{S}$	0.5410	-	0.211	39.97	0.59	5.13

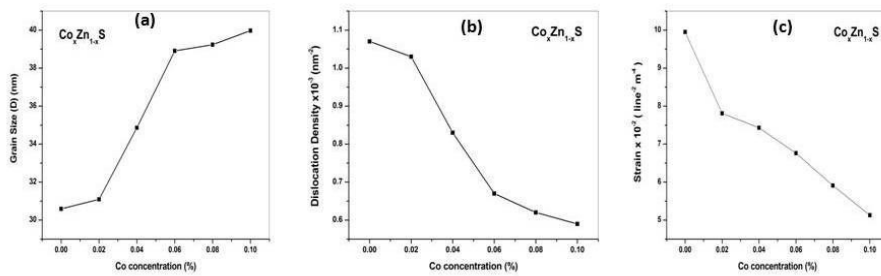


Fig 2. Variation of cobalt concentration Vs (a) Grain Size (D) (b) Dislocation Density (δ) (c) Strain (ϵ) of $\text{Co}_x\text{Zn}_{1-x}\text{S}$ compound with $x=0-0.1$.

3.2 Optical Characterization

The UV-Absorption spectra of $\text{Co}_x\text{Zn}_{1-x}\text{S}$ samples were recorded using SHIMADZU, UV-3100 spectrometer. The prepared sample were powdered and suspended in glycerol (stirred for half and hour using magnetic stirrer for the particles to spread uniformly) and their optical absorption spectrum was recorded at room temperature over the wavelength range 200 to 800 nm. Fig.3 shows the absorption spectra of $\text{Co}_x\text{Zn}_{1-x}\text{S}$ ($x=0-0.1$) samples. Also it is observed from the graph that the strongest absorption peak appears at about 297 nm (not shown in the Fig.3) in all the samples of $\text{Co}_x\text{Zn}_{1-x}\text{S}$ ($x=0-0.1$). The peaks which were observed in all the samples are assigned as typical internal d-d transitions of Co ions. This attributes Co^{2+} is incorporated at the Zn^{2+} lattice site in ZnS [28].

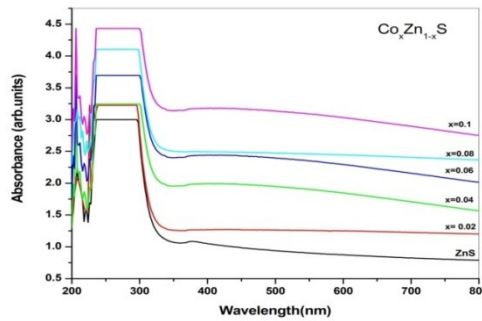


Fig. 3 UV-absorption spectra of $\text{Co}_x\text{Zn}_{1-x}\text{S}$ ($x=0-0.1$) compound.

The fundamental absorption, which corresponds to electron excitation from the valence band to conduction band, can be used to determine the value of optical band gap. The relation between the absorption coefficient (α) and the incident photon energy ($h\nu$), known as Tauc's relation, can be written as [29].

$$\alpha(h\nu) = A(h\nu - E_g)^n \quad (6)$$

Where A is a constant, E_g is the band gap and n assumes values 1/2, 2, 3/2 and 3 for allowed direct, allowed indirect, forbidden direct and forbidden indirect transitions respectively. Here $n=1/2$ is considered as the compound possesses allowed direct transition [30]. The direct band gap energy of a sample can be determined by the extrapolation of the linear regions on the energy axis ($h\nu$).

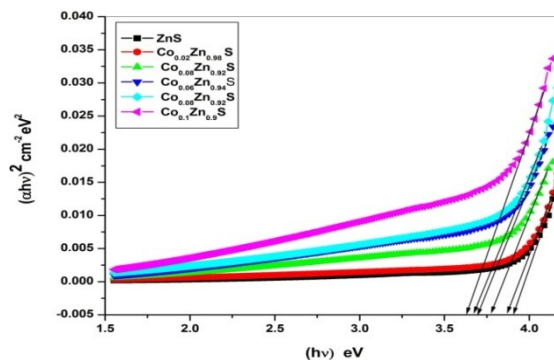


Fig 4. Plot of $(h\nu)$ eV versus $(\alpha h\nu)^2 \text{ cm}^{-2} \text{ eV}^2$ of $\text{Co}_x\text{Zn}_{1-x}\text{S}$ (0-0.1) compound.

Fig. 4 shows the direct band gap calculation of $\text{Co}_x\text{Zn}_{1-x}\text{S}$ compounds by extrapolating the straight line region of the plot drawn between $(\alpha h\nu)^2$ and $(h\nu)$ to the energy axis. The values of energy gap thus calculated for all $\text{Co}_x\text{Zn}_{1-x}\text{S}$ compounds are given in the Table.3. As seen from Fig.4 and Table 3, the band gap value decreased

from 3.91 to 3.62eV with increases in cobalt concentration (x). The graphical variation of E_g with cobalt composition is shown in Fig.5. The decrease in band gap with cobalt concentration can be attributed to a real change in band strength between ZnS and CoS, change in atomic distances and grain size. This result is in agreement with the published literature. For low concentrations of cobalt, optical band gap of the material changed from 3.91-3.62 eV. By virtue of the value of their band gap they come under higher band gap materials. Therefore, they are the suitable material for fabrication of electroluminescent devices and solid state solar window layers.

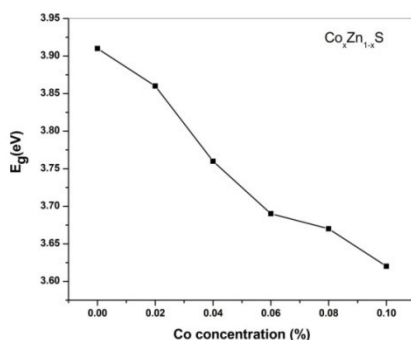


Fig. 5 Cobalt concentration (x) Vs E_g (eV) of $\text{Co}_x\text{Zn}_{1-x}\text{S}$ (0-0.1) compound

TABLE 3. The energy band gap values of $\text{Co}_x\text{Zn}_{1-x}\text{S}$ (x=0-0.1) compound.

$\text{Co}_x\text{Zn}_{1-x}\text{S}$ (x=0-0.1)	Energy band gap (E_g) eV
ZnS	3.91
$\text{Co}_{0.02}\text{Zn}_{0.98}\text{S}$	3.86
$\text{Co}_{0.04}\text{Zn}_{0.96}\text{S}$	3.76
$\text{Co}_{0.06}\text{Zn}_{0.94}\text{S}$	3.69
$\text{Co}_{0.08}\text{Zn}_{0.92}\text{S}$	3.67
$\text{Co}_{0.1}\text{Zn}_{0.9}\text{S}$	3.62

3.3. Elemental Analysis

In material characterization, it is important to determine how an element is distributed laterally and to find the inclusions on the surface. This is most conveniently done by using a focused probe of x-rays or ion that is scanned over the surface and the characteristic elemental signals are used to produce an elemental map of the surface. Fig. 6 shows the EDAX spectrum of $\text{Co}_x\text{Zn}_{1-x}\text{S}$ (x=0, 0.02, 0.1). The spectrum confirms the presence of Zn, S, Co, and O atoms that are present in the compound. A small amount of oxygen present in the compound may be due to the inclusion into the compound either from the atmosphere or from aqueous medium of the solution. This shows the formation of the compound with slight hydrous nature.

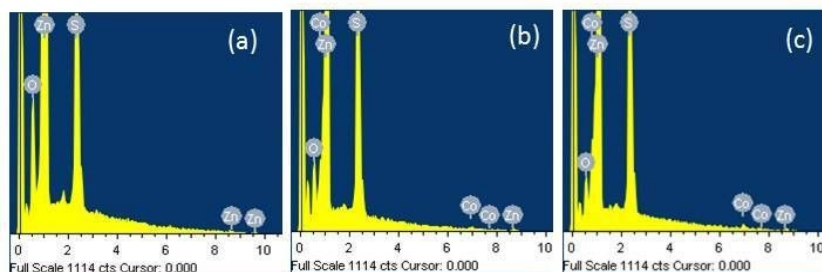


Fig 6. EDAX spectra of (a) ZnS (b) $\text{Co}_{0.02}\text{Zn}_{0.98}\text{S}$ (c) $\text{Co}_{0.1}\text{Zn}_{0.9}\text{S}$ compounds.

3.4. Morphological studies

Scanning Electron Microscope (SEM) study is the powerful tool to study the surface morphology especially to observe the top and the cross-sectional views. Fig.7 shows the typical SEM micrographs of the $\text{Co}_x\text{Zn}_{1-x}\text{S}$ (x=0, 0.02, 0.06, 0.1) compounds. Formation of nearly spherical agglomeration in the range 100-200 nm size is evident from the micrographs. It is also noticed that, as the cobalt concentration(x) increases, the morphology of the agglomerations tend to become more spherical with slight increase in the size.

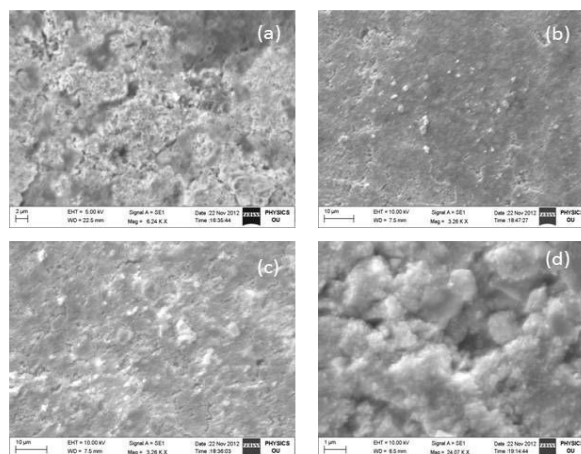


Fig 7. SEM micrographs of (a) ZnS (b) $\text{Co}_{0.02}\text{Zn}_{0.98}\text{S}$ (c) $\text{Co}_{0.06}\text{Zn}_{0.94}\text{S}$ (d) $\text{Co}_{0.1}\text{Zn}_{0.9}\text{S}$ compounds.

3.5. FTIR Spectra

The infrared spectroscopic studies of the samples were done using BRUKER optics, Germany spectrometer in the wave number range $400\text{-}4000\text{ cm}^{-1}$. The FTIR spectrum of ZnS is shown in Fig.8(a) In this spectrum the bands at 3814 cm^{-1} , 3227 cm^{-1} correspond to the O-H vibrations of water molecules, the peak at 2870 cm^{-1} correspond to the C-H bond, the band at 2369 cm^{-1} show the presence of CO_2 in the sample [31]. The band at 1578 cm^{-1} corresponds to the hydroxyl group present in the sample. The acetate bands of C-O are observed at 1215 cm^{-1} . The band at 630 cm^{-1} corresponds to the vibration of Zn-S [32]. Fig.8 (b,c) shows the FTIR spectrum of $\text{Co}_x\text{Zn}_{1-x}\text{S}$ ($x=0.02, 0.1$). In this the absorption bands near 3458 cm^{-1} represent O-H mode, those at 2956 cm^{-1} are C-H mode, and the peaks near $1400\text{-}1700\text{ cm}^{-1}$ are the C=O stretching mode [33]. The absorption peaks at 663 cm^{-1} corresponds to the vibrations of Zn-S. The peaks formed at $700\text{-}900\text{ cm}^{-1}$ are attributed to the bond between Cobalt and Sulphur [34]. Also we can observe additional peaks in the wave number region $600\text{-}1300\text{ cm}^{-1}$ which is the region of Zn-S and Co-S bonding which again represent the presence of additional phases at higher concentration of doping [35].

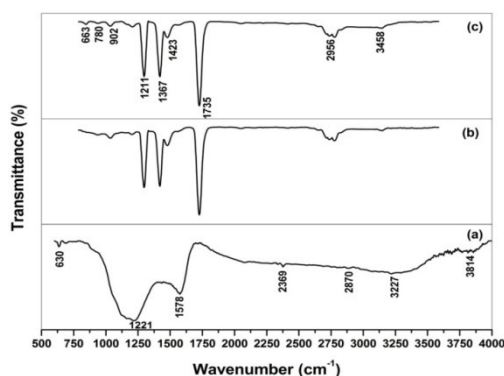


Fig 8. FTIR spectra of (a) ZnS (b) $\text{Co}_{0.02}\text{Zn}_{0.98}\text{S}$ (c) $\text{Co}_{0.1}\text{Zn}_{0.9}\text{S}$ compounds.

IV. Conclusions

1. $\text{Co}_x\text{Zn}_{1-x}\text{S}$ compounds were synthesized by the co-precipitation technique.
2. The XRD and SEM studies showed that $\text{Co}_x\text{Zn}_{1-x}\text{S}$ compound has Polycrystalline nature and its crystallinity varied from hexagonal to near cubic with the increase in cobalt concentration from ($x=0\text{-}0.1$) and surface properties of the compound improved by increasing copper concentration(x).
3. EDAX spectrum confirmed the chemical homogeneity of the samples and also showed that the atomic percentages present were as per the constituents taken in the compound.
4. UV-Visible spectrum confirmed the decrease of band gap with increasing cobalt concentration (x) in $\text{Co}_x\text{Zn}_{1-x}\text{S}$ compound.
5. The grain size in $\text{Co}_x\text{Zn}_{1-x}\text{S}$ has increased and dislocation density and strain values have decreased with the increase in cobalt concentration (x). And all these variations are observed to be non-linear.
6. The vibrational bands evaluated from FTIR spectra confirmed that the cobalt is induced into the lattice replacing Zinc.

Acknowledgements

The author thank The Head, Department of Physics, Osmania University, Hyderabad and also The Director, CFRD, Osmania University, Hyderabad-500007 for providing facilities.

References

- [1] Sihai Chen, Takashi Ida and Keisaku Kimura, Thiol-Derivatized AgI Nanoparticles: Synthesis, Characterization, and Optical Properties, *The Journal of Physical Chemistry B*, 102 (32), 1998, 6169–6176.
- [2] S. Das Sarma, Spintronics, A new class of device based on the quantum of electron spin, rather than on charge, may yield the next generation of microelectronics, *American Scientist*, 89, 2001, 516-523.
- [3] H. Ohno, F. Matsukura and Y. Ohno, General Report Semiconductor Spin Electronics, *J SAP International*, 5, 2002, 4.
- [4] S. J. Pearton, C. R. Abernathy, D. P. Norton, A. F. Hebard, Y. D. Park, L. A. Boatner and J. D. Budai, Advances in wide bandgap materials for semiconductor spintronics, *Materials Science and Engineering R* 40, 2003, 137–168.
- [5] J. K. Furdyna, Diluted magnetic semiconductors, *Journal of Applied Physics* 64(4), 1988, R 29.
- [6] M. Romcevic, N. Romcevic, R. Kostic, L. Klopotoski, W. D. Dobrowolski, J. Kossut, and M. I. Comor, Photoluminescence of highly doped $\text{Cd}_{1-x}\text{Mn}_x\text{S}$ nanocrystals, *Journal of Alloys and Compounds*, 497(1-2), 2010, 46-51.
- [7] K. Siva Kumar, A. Divya and P. Sreedhara Reddy, Synthesis and characterization of Cr doped CdS nanoparticles stabilized with polyvinylpyrrolidone, *Applied Surface Science*, 257(22), 2011, 9515-9518.
- [8] K. Takamura, F. Matsukura, D. Chiba and H. Hono, Magnetic properties of (Al,Ga,Mn)As, *Applied Physics Letters*, 81(14), 2002, 2590-2592.
- [9] H. Lu and S.Y. S. Chu, The mechanism and characteristics of ZnS-based phosphor powder, *Journal of Crystal Growth*, 265, 2004, 476-481.
- [10] J. Dai, Z. Jiang, W. Li, G. Bian and Q. Zhu, Solvothermal preparation of inorganic-organic hybrid compound of $[(\text{ZnS})_2(\text{en})]_n$ and its application in photocatalytic degradation, *Materials Letters*, 55(6), 2002, 383-387.
- [11] J. F. Reber and K. Meier, Photochemical production of hydrogen with zinc-sulfide suspensions, *J. Phys. Chem.* 88(24), 1984, 5903-5913.
- [12] H. Yin, Y. Wada, T. Kitamura and S. Yanagida, Photoreductive dehalogenation of halogenated benzene derivatives using ZnS or CdS nanocrystallites as photocatalysts. *Environ. Sci. Technol.*, 35 (1), 2001, 227-231.
- [13] J. L. Birman, Simplified LCAO method for zinc blende, wurtzite and mixed crystals structures, *Phys. Rev.* 115, 1959, 1493-1505.
- [14] T. Arai, S. Senda, Y. Sato, H. Takahashi, K. Shinoda, B. Jayadevan and K. Tohji, *Chem. Mater.* 20 (2008) 1997.
- [15] S. Bhattacharya and D. Chakravorty, Electrical and magnetic properties of cold compacted iron-doped zinc sulfide nanoparticles synthesized by wet chemical method, *Chemical Physics Letters*, 444, 2007, 319-323.
- [16] S. Biswas, S. Kar and S. Chaudhuri, Optical and magnetic properties of manganese- incorporated zinc sulfide nanorods synthesized by a solvothermal process, *J. Phys. Chem. B* 109(37), 2005, 17526-30.
- [17] I. Sarkar, M.K. Sanyal, S. Kar, S. Biswas, S. Banerjee, S. Chaudhuri, S. Takeyama, H. Mino and F. Komori, Ferromagnetism in zinc sulfide nanocrystals: Dependence on manganese concentration, *Phys. Rev. B* 75, 2007, 224409(5 pages) .
- [18] J. Yu, H. Liu, Y. Wang and W. Jia, Hot luminescence of Mn^{2+} in ZnS nanocrystals, *Journal of Luminescence*. 79(3), 1998, 191-199.
- [19] J. Huang, Y. Yang, S. Xue, B. Yang, S. Liu and J. Shen, Photoluminescence and electroluminescence of ZnS:Cu nanocrystals in polymeric networks, *Applied Physics Letters*, 70, 1997, 2335-2337.
- [20] W. Jian, J. Zhuang, D. zhang, J. Dai, W. Yang and Y. Bai, Synthesis of highly luminescent and photostable ZnS:Ag nanocrystals under microwave irradiation, *Materials Chemistry and Physics*, 99(2-3), 2006, 494-497.
- [21] S. H. Yu and M. Yoshimura, Shape and Phase Control of ZnS Nanocrystals: Template Fabrication of Wurtzite ZnS Single-Crystal Nanosheets and ZnO Flake-like Dendrites from a Lamellar Molecular Precursor $\text{ZnS} \cdot (\text{NH}_2\text{CH}_2\text{CH}_2\text{NH}_2)_{0.5}$, *Advanced Materials*, 14(4), 2002, 296-300.
- [22] Z. X. Deng, C. Wang, X. M. Sun and Y. D. Li, Structure-directing coordination template effect of ethylenediamine in formations of ZnS and ZnSe nanocrystallites via solvothermal route, *Inorganic Chemistry*, 41(4), 2002, 869-873.
- [23] F. Gode, C. Gumus and M. Zor, Investigations on the physical properties of the polycrystalline ZnS thin films deposited by the chemical bath deposition method, *Journal of Crystal Growth*, 299(1), 2007, 136-141.
- [24] V. Laxminarasimha Rao, T. Shekhar and M. Nagabhushanam, Synthesis and Characterisation of $\text{Cu}_x\text{Zn}_{1-x}\text{S}$ Polycrystalline Semiconductors by Co-Precipitation Method, *International Journal of Materials Science and Technology*. 3(1), 2013, 27-40.
- [25] B. D. Cullity and S. R. Stock, *Elements of X-Ray Diffraction* (Prentice-Hall, 2001).
- [26] M. Ali Yildirim, The effect of copper concentration on structural, optical and Dielectric properties of $\text{Cu}_x\text{Zn}_{1-x}\text{S}$ thin films, *Optics Communications*, 285(6), 2012, 1215-1220.
- [27] M. Ashraf, S. M. J. Akhtar, A. F. Khan, Z. Ali and A. Qayyum, Effect of annealing on structural and optoelectronic properties of nanostructured ZnSe, *Journal of Alloys and Compounds*, 509(5), 2011, 2414-2419.
- [28] N. Volbers, H. Zhou, C. Knies, D. Pfisterer, J. Sann, D. M. Hofmann and B. K. Meyer, Synthesis and characterization of $\text{ZnO}:\text{Co}^{2+}$ nanoparticles, *Applied Physics A*. 88, 2007, 153-155.
- [29] A. Rahdar, V. Arbabi and H. Ghanbari, Study of Electro-Optical Properties of ZnS Nanoparticles Prepared by Colloidal Particles Method, *World Academy of Science, Engineering and Technology*, 61(1), 2012, 657-659.
- [30] D. Duygu Dogan, Y. Caglar, S. Ilcan and M. Caglar, Investigation of structural, morphological and optical properties of nickel zinc oxide films prepared by sol-gel method, *Journal of Alloys and Compounds*, 509(5), 2011, 2461-2465.
- [31] K. Ashwini, C. Pandurangappa and B. M. Nagabhushana, Synthesis and optical properties of undoped and Eu-doped ZnS nanoparticles, *Physica Scripta*, 85(6), 2012, 065706 (5pp).
- [32] Zhang Rui, Liu Yingbo and Sun Shuqing, Synthesis and characterization of high-quality colloidal Mn^{2+} -doped ZnS nanoparticles, *Optical Materials*, 34(11), 2012, 1788-1794.
- [33] M. Vafaei and M. G. Sasani, Preparation and characterization of ZnO nanoparticles by a novel sol-gel route, *Materials Letters*. 61(14-15), 2007, 3265-3268.
- [34] K. Byrappa, A. K. Subramani, S. Ananda, K. M. Lokanatha Rai, M. H. Sunitha, B. Basavalinga and K. Soga, Impregnation of ZnO onto activated carbon under hydrothermal conditions and its photocatalytic properties, *Journal of Materials Science*. 41(5), 2006, 1355-1362.
- [35] Muhammad Ahsan Shafique, Saqlain A. Shah, Muhammad Nafees, Khalid Rasheed and Riaz Ahmad, Effect of doping concentration on absorbance, structural, and magnetic properties of cobalt-doped ZnO nano-crystallites, *International Nano Letters*, 2:31, 2012, 1-7.